

Chapter 4

Results and Discussion

4.1 Solution Deposition Method

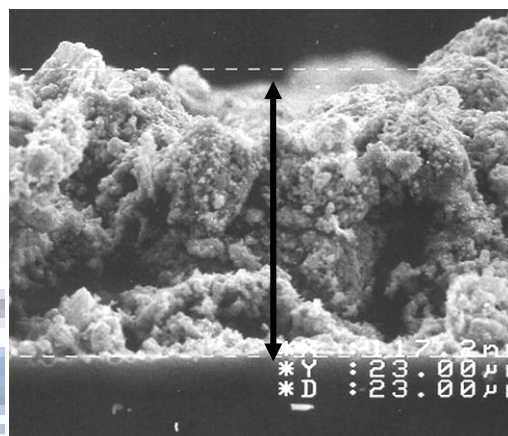
4.1.1 Pretreatment Time of Hydrogen Plasma

In Fig. 4.1, it showed the surface morphology of the as-deposited specimens with catalysts synthesized by solution deposition method. The thickness of the specimen with nickel (Ni) /silver (Ag) layer was about 23 μm . A few catalysts and impurities appeared on the surface and the surface was very uneven. Fig. 4.2 showed the SEM images of various surface changes after different time of hydrogen plasma pretreatment under the power of 150 W and the work pressure of 6 Torr. Compared with the Fig. 4.1, the amounts of catalysts increased with the pretreatment time. But after 30min, the catalysts aggregated together, and the amounts of catalysts decrease. The diameter of catalysts also increased with the pretreatment time from 50 nm to about 100 nm.

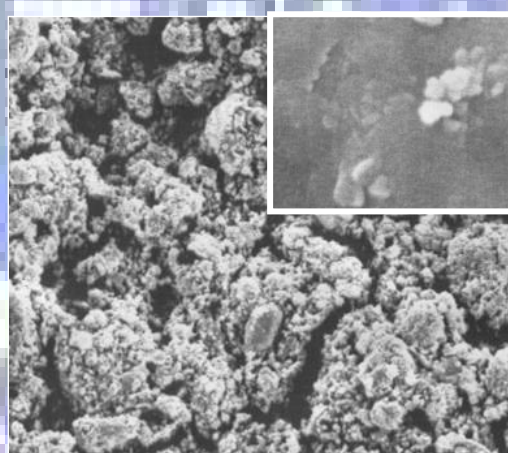
In this study, we used the pretreatment time of 5 min, not 15 min, 30 min, or 45 min. Because during the growth of carbon nanotubes (CNTs), the hydrogen plasma still bombarded the surface of specimens. The catalysts on the surface were activated so that we did not increase the pretreatment time to activate the surface.

4.1.2 Effect of Methane Concentration

After H_2 pretreatment for 5 min, various parameters were introduced to find an optimal growth condition at low temperature. Fig. 4.3 showed the SEM images of various H_2/CH_4 ratio for 30 min. Under fixing the methane flow rate (10 sccm), the H_2 gas flow rate was changed from 40 sccm to 10 sccm. The graphitic carbon nanotubes



(a)



(b)

Fig. 4.1 SEM images of the as-deposited specimens with catalysts synthesized by screen printing method, (a) cross-section view; (b) top view. The inset diagram is the magnification.

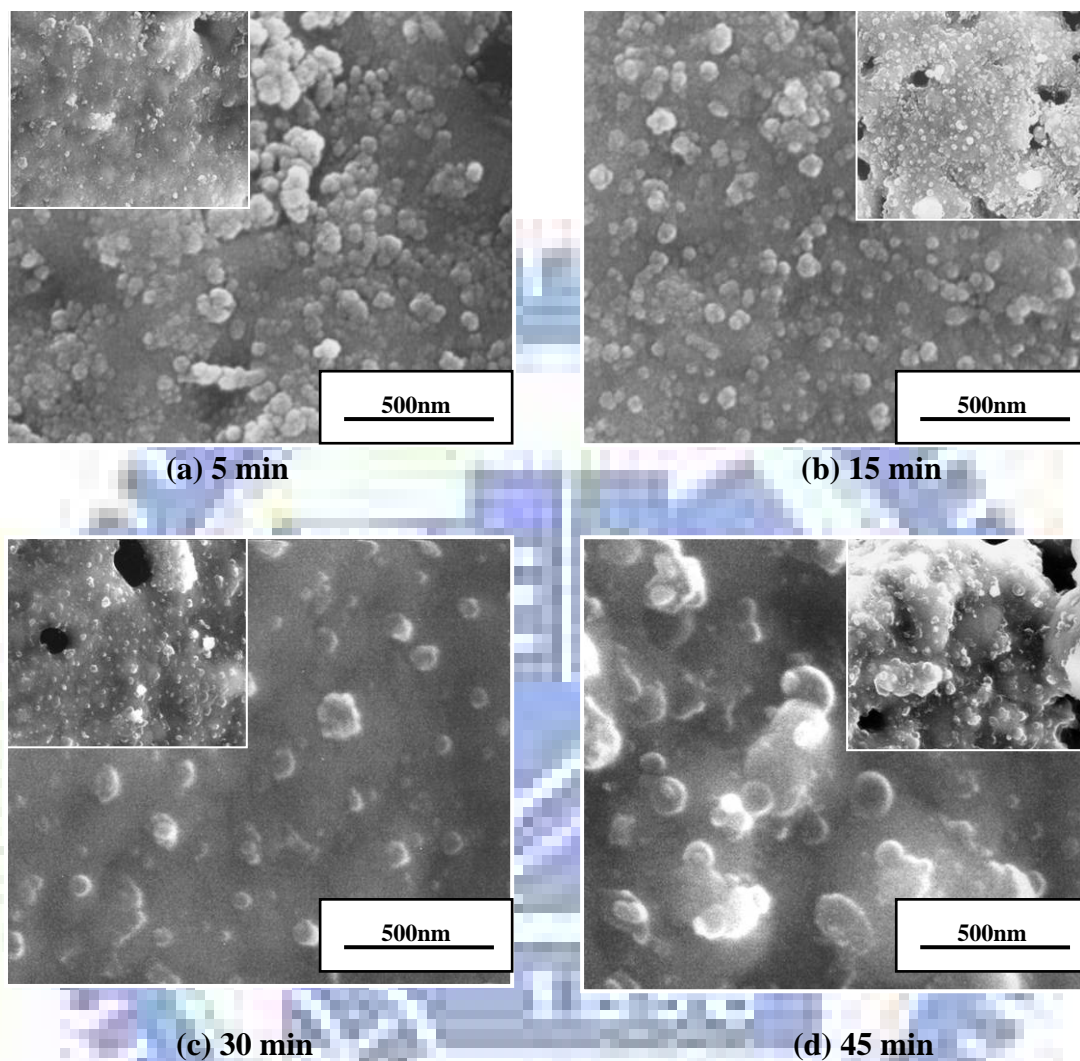


Fig 4.2 SEM images of various surface of hydrogen plasma pretreatment for different time: (a) for 5 min, (b) for 15 min, (c) for 30 min, (d) for 45 min. The inset diagram is the magnification.

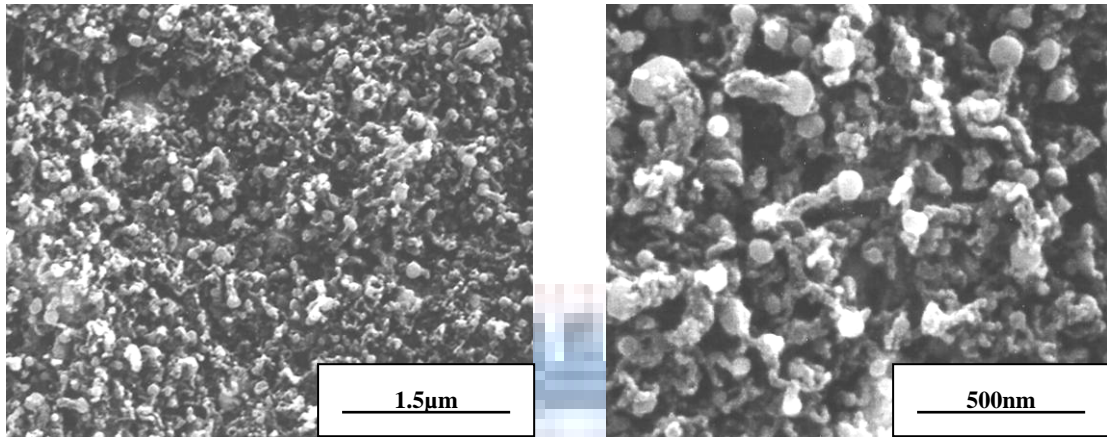
were uniformly grown on a large area ($1 \times 1 \text{ cm}^2$) with high density.

As the concentration of carbon source increase, the diameter and the length also increases in our experiments. The diameter of carbon nanotubes obviously increases from 50 nm to 100 nm, and the length also increases from 250 nm to about 1 μm . So, for low temperature growth, the high concentration of carbon source is suitable.

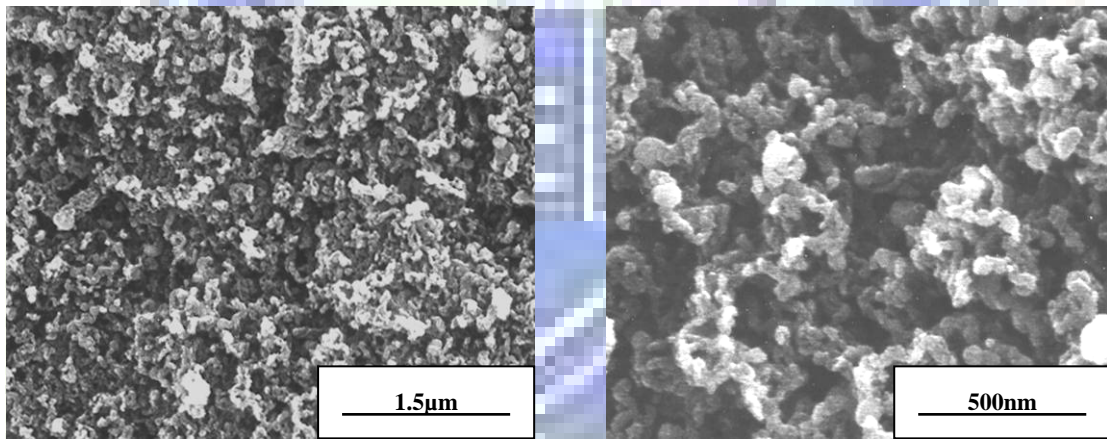
Table 4.1 and fig. 4.4 showed the Raman data of the multiwall carbon nanotubes grown by microwave plasma-enhanced CVD in $\text{H}_2\text{-CH}_4$. A typical graphite vibration mode G-line at 1595 cm^{-1} and a disordered carbon mode D-line at 1316 cm^{-1} appears in the spectrum. The 1595 cm^{-1} peak indicates the formation of graphitized structure, and the 1316 cm^{-1} peak origination may be attributed to defects in the curved graphite sheets, nanotubes tips and amorphous carbon film covering the template surface as mentioned above. The I_D/I_G ratio decreased with increasing methane concentration. The results implied the amounts of amorphous carbonaceous by product adhered to wall and defective structure in multiwall layer decreased. The results of I_D/I_G ratio is not the same with the growth of diamond films [54,55] or carbon nanotubes [56] at high temperature. The reason is that in our experiments the pressure and flow rate of gas were low, so the carbon species became rare on the plasma. Thus, only by increasing the concentration of carbon source, the carbon nanotubes just had enough carbon atoms to form sp^2 or sp^3 bonding species.

4.1.3 Effect of Total Flow Rate

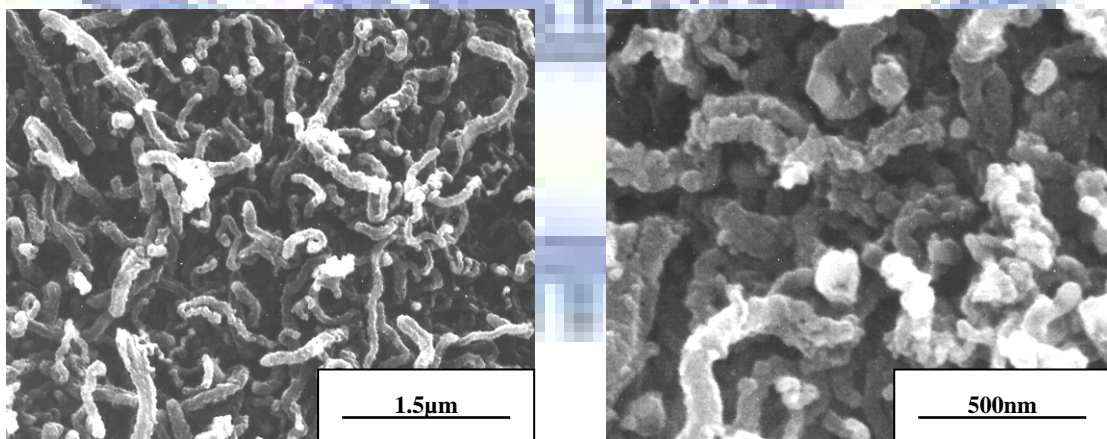
In fig 4.5, it showed Raman spectrum of different flow rate and data of I_D/I_G ratio. As the flow rate H_2/CH_4 was equal to 5/5 sccm (10 sccm), the peaks showed that only carbon films were grown, owing to no peaks appearing at 1316 cm^{-1} (D-line) and at 1595 cm^{-1} (D-line). When the flow rate of gas was increased, the carbon nanotubes were grown, owing to two peaks appearing at 1316 cm^{-1} and 1595 cm^{-1} . However, the



(a) 40/10



(b) 20/10



(c) 10/10

Fig. 4.3 SEM images of different methane concentration under the growth condition at 150 W and 6 Torr for 30 min, (a) $H_2/CH_4=40/10$ sccm, (b) $H_2/CH_4=20/10$ sccm, (c) $H_2/CH_4=10/10$ sccm.

	40/10	20/10	10/10
D band	382400	523950	328869
G band	120180	168490	141388
I_D/I_G	3.18189	3.10968	2.326

Table 4.1 the data of Raman spectra under different mathan concentration at power of 150 W and the pressure of 6 Torr for 30 min (sccm).

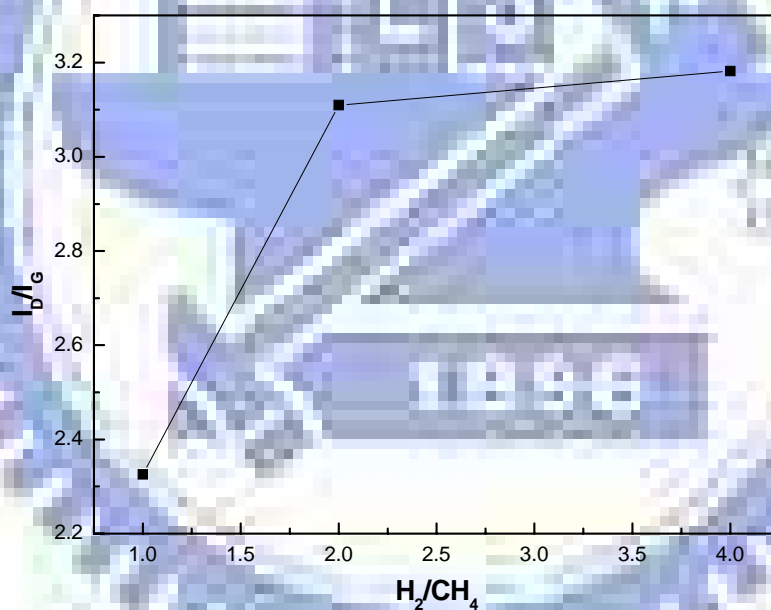


Fig. 4.4 I_D/I_G ratio varied with H_2/CH_4 ration of 150 W and 6 Torr for 30 min.

I_D/I_G ratio of 25/25 sccm (50 sccm) was decreased compared with 5/5 sccm. It implied that a better graphitization only on the flow rate of 5/5 sccm (10 sccm). It was interesting that the temperature of the substrate increased with the total flow rate was decreased. The temperature of 5/5 sccm was about 620 °C higher than 10/10 sccm (about 555 °C) and 25/25 sccm (about 510 °C) and the sample of 5/5 sccm was bending at 620 °C. Hereafter, the flow rate of 10/10 sccm was used as growth CNTs either on solution deposition method or sol-gel method.

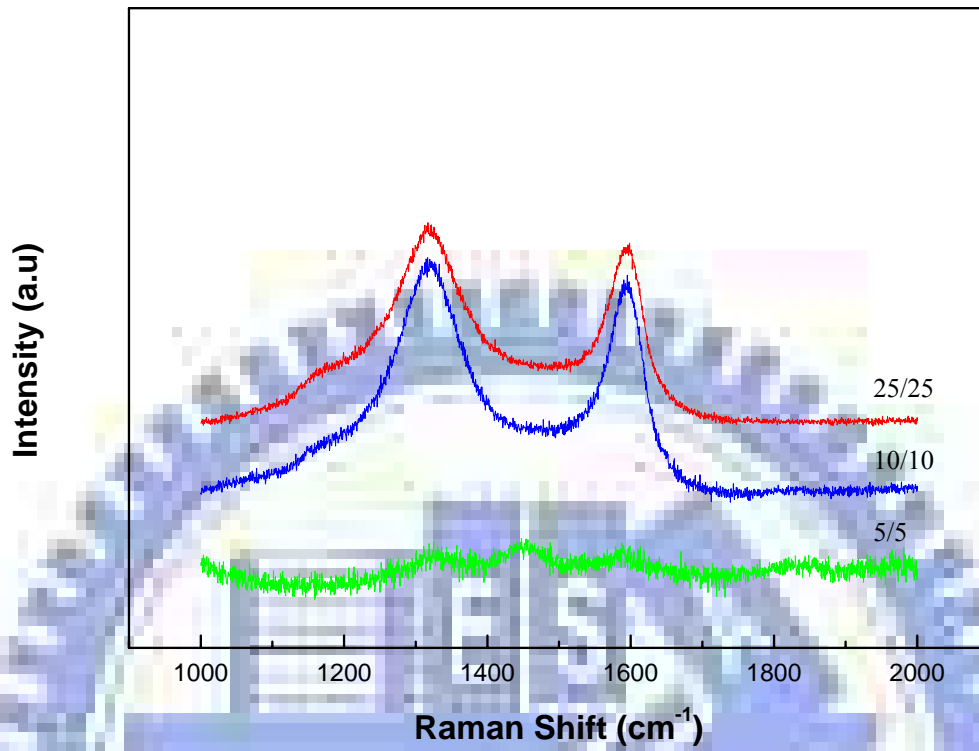
4.1.4 Effect of MPCVD Power

For growing excellent qualities of carbon nanotubes, the MPCVD power were raised from 150 W to 200 W. Undoubtedly, the plasma temperature also increased from about 555 °C to about 625 °C measured by IR thermocouple. Fig. 4.6 showed the SEM images with different H_2/CH_4 under the power of 200 W and the pressure of 6 Torr for 30 min. We could clearly see the diameter and length of carbon nanotubes increased with hydrogen contents in H_2/CH_4 decreasing from 40/10 sccm to 10/10 sccm. This result was the same as mentioned in section 4.1.1.

Interesting, in table 4.2, also compared the fig. 4.10 with fig. 4.5, the I_D/I_G ratio decrease as the power was increased from 150 W to 200 W. It implied that the quality of carbon nanotubes became better. But it was a pity that over the MPCVD power of 200 W the sample damaged and bent by heat at about 625 °C for 30 min. It meant that the sample of the glass substrate was over-heating.

4.1.5 Effect of Growth Time of Carbon Nanotubes

In fig. 4.7 it showed the SEM images of surface morphology under the growth condition of gas flow rate of 10/10 (H_2/CH_4 , sccm) at the power of 150 W and the pressure of 6 Torr. The length and diameter increased with the growth time. This was



	5/5	10/10	25/25
I_D/I_G	—	2.33	2.42
T(°C)	620	555	510

Fig 4.5 Raman spectrum varied with different flow rate and data of I_D/I_G ratio and I_D/I_G datd.

because carbon species of plasma had enough time to deposit at the wall of tubes. But as the time was over 30 min, like 45 min and 60 min, amorphous carbons accumulated on the surface of the sample, and the sample damaged and bent by appearance. The reason was that as the time was over 30 min, the ions of plasma continued hitting the surface. Kinetic energy transformed into thermal energy. And this circumstance obliged the heat to accumulate on the surface of the sample.

From the table 4.3 and fig. 4.8, the I_D/I_G ratio increased for 45 min and 60 min compared with 30 min. The optimal growth time was 30 min due to the minimum I_D/I_G ratio. These observations suggest that amorphous carbon particles attach to the outer wall of carbon nanotubes were etched by hydrogen plasma. After the growth time over 30 min, etching rate smaller than the deposited rate of carbon atoms, the amorphous carbon started to pile up on the outer wall of carbon nanotubes, as confirmed in fig 4.7.

4.1.6 TEM Analysis of Carbon Nanotubes

Fig. 4.9 showed the TEM images of CNTs in our experiments. The morphology of carbon nanotubes was the same no matter on any growth conditions. Thus the uniformity and reproduction of carbon nanotubes in this study were undoubted. From the TEM images, we could see two kinds of CNTs grown on the samples. One was herringbone-like structure with a diameter of about 50 nm showed in fig. 4.9 (a), and the other one is like nanofiber with a diameter of about 45 nm showed in fig. 4.9 (b). Especially the herringbone-like structure consisted of several graphitic shells with a central hollow region. A metal particle at the tip of CNTs is visible in the two structure, and two structure tubes both showed curved structures. Catalytic metal particles were located at the tips, indicating the tip growth mode. Since the growth temperature was very low (below 650 °C), carbon atoms deposited at the edge of the

tubes do not have enough time and kinetic energy to diffusion, forming defective edges with pentagons and heptagons which eventually induced bending in carbon nanotubes [57]. Each nanotube was terminated by a metal cap, which was also observed in other CVD experiments.

In fig. 4.10 high-resolution TEM analysis showed that the degree of crystallinity of the carbon nanotubes grown at low temperature. As showed in this figure, the CNTs revealed multiwall structure. And the metal particle was embedded in the tube by well-graphite layer at the tip in fig. 4.10 (a). From the EDX analysis of TEM in fig.4.11, the metal particle at the tip was Ni., so the Ag was not suitable catalyst for growing CNTs. The HRTEM characteristics also indicated that there were many amorphous carbons on the surface of the tubes. And in fig. 4.14 (b), the fiber-like structure consisted of several graphitic shell and exhibited similar “loop”. The symmetry of the carbon nanotubes was not good.

4.1.7 Field Emission characteristics

Fig.4.12 showed the I-V characteristics, an anode was placed directly above the CNTs using a 100 μm spacer. The sample was grown at 555 $^{\circ}\text{C}$ for 30 min under 150 W and 6 Torr. A turn-on field, E_{t0} , is defined as the field to give an emission current density of 10 $\mu\text{A}/\text{cm}^2$. The turn on field values of 3.2 $\text{V}/\mu\text{m}$ was found. The inset diagram shows the Fowler-Nordheim plot of I-V curve. And The F-N plots, $\ln(I/E^2)$ vs $1/E_0$, were expected to be a straight line, indicating that field electron emission is intrinsically driven by the electric field. But the plots of CNTs had two components, as shown in the inset. A larger slope appears at the lower fields and a larger slope at higher fields. The two section FN plot is contributed to the fact that electrons can emit not only from the top of the tubes but also from the side, which many graphite edges exist from the open end of the nanobells [58,59]. The very low turn on field at 555 $^{\circ}\text{C}$

could be attributed to large field enhancement effect. Also, it has been accepted that hydrogen plasma treatment on amorphous carbon is an effective way to improve the emission characteristics.

The field enhancement factor β were derived from the slops by assuming a work function of CNTs as 5 ev. The field enhancement factor β was 3400.

